LABORATORI NAZIONALI DI FRASCATI
SIS – Pubblicazioni

LNF–95/050 (P)
11 Settembre 1995

Quasi–Elastic Scattering in the Inclusive (^{3}He, t) Reaction

Neelima G. Kelkar
INFN – Laboratori Nazionali di Frascati, P.O. Box 13, I 00044–Frascati (Roma) Italy

B.K. Jain
Nuclear Physics Division, Bhabha Atomic Research Centre, Bombay–400085, India

Abstract

The triton energy spectra of the charge-exchange ^{12}C(^{3}He,t) reaction at 2 GeV beam energy are analyzed in the quasi-elastic nucleon knock-out region. Considering that this region is mainly populated by the charge-exchange of a proton in ^{3}He with a neutron in the target nucleus and the final proton going in the continuum, the cross-sections are written in the distorted-wave impulse approximation. The t-matrix for the elementary exchange process is constructed in the DWBA, using one pion- plus rho-exchange potential for the spin-isospin nucleon- nucleon potential. This t-matrix reproduces the experimental data on the elementary pn $\rightarrow$np process. The calculated cross-sections for the ^{12}C(^{3}He,t) reaction at 2^o to 7^o triton emission angle are compared with the corresponding experimental data, and are found in reasonable overall accord.

PACS.: 13.75.-n; 25.55.-e

Submitted to Physical Review C

1 Introduction

Because of the easy transferability of sufficient energy in the intermediate energy nuclear collisions to the nucleus, and the reduced effect of the Pauli blocking, the quasi-free scattering forms a major portion of the reactive content in nuclear cross-sections at these energies. In experiments, this fact is manifested by a broad bump in the ejectile energy spectrum around $\omega = q^2/2m^*$, where (ω, q) is the four momentum transfer to the nucleus (m^* being the effective mass of the nucleon). The width of this bump is correlated to the momentum spread of the nucleon in the nucleus. In earlier times, this aspect was exploited much to gather directly the information about the single particle aspect, in particular the shell model, of the nucleus through the study of the inclusive (p,p′), (e,e′) reactions, and the exclusive (p,2p), (e,e′p) [1], and other reactions of similar type. In recent years, however, the focus on similar studies has shifted to the charge-exchange reactions, like (p,n), (^{3}He,t) in the quasi-free region [2,3]. This has happened because of the discovery of strong Gamow-Teller excitations in these reactions and a rather simple (Born term) description of the spin-isospin piece of the N-N interaction in terms of a one- pion- and a rho-exchange interaction [4]. It is felt that the study of these reactions in the quasi-free region, like the earlier quasi-free knock-out studies, would provide an opportunity to explore the single particle spin-isospin response of the nucleus. This response, due to pi- and a rho-meson-exchange, contains longitudinal as well as the transverse components. Going beyond the single particle aspect, one expects that these studies may also explore the particle-hole correlations in the quasi-free region. Theorists predict [5] that the particle-hole correlations, apart from modifying the magnitudes, shift the longitudinal response towards the lower excitation energy and the transverse response towards the higher excitation energy. In addition, it is also known that these correlations also renormalize the propagation of pions in the nuclear medium. Because of this, the study of the spin-isospin nuclear response to various external probes has been a topic of great interest over the past decade. An extensive experimental study of the (^{3}He,t) reaction has been carried out at Saturne [6], and the (p,n) reaction at Los Alamos [2]. Theoretically too, several efforts have been made to study these reactions. Alberico et al. [7] have developed a random phase approximatiom theory (RPA) of the spin-isospin nuclear surface response and studied the contrast between the spin-longitudinal (R_L) and spin-transverse

(R_T) part of the nuclear response. Their predictions are for nuclear matter and use a ($\pi + \rho + g'$) model for the interaction. Ichimura et al. [8] have improved upon this method and have calculated R_L and R_T by the continuum RPA with the orthogonality condition. They treat the nucleus as of finite size and present the cross-sections for ^{40}Ca(p,p′) reaction at $E_p = 500$ MeV using the distorted wave impulse approximation. However, notwithstanding these efforts, Bertsch et al. [9], while discussing a number of experiments in a recent critical review of this field, find that the effect of the residual particle-hole correlations seen in the experiments in the quasi-free region is much smaller than expected.

Considering the above observation of Bertsch et al. [9] as an indication of the weakness of the correlations (whatever may be the reason), in the present paper we study the quasi-elastic peak region as being populated by the charge-exchange knock-out of a neutron in the target nucleus. The motivation for this work is to explore the extent upto which the experimental data could be accounted by the independent particle framework alone. We have done the calculations in the DWIA, where the interaction of the mass 3 particles in the continuum with the nucleus is incorporated through the use of distorted waves. As a typical case, we analyse the data on the ^{12}C(^{3}He,t) reaction at 2 GeV beam energy [3]. Specifically, we assume that the quasi-free region in this reaction is populated by the ^{12}C(^{3}He,tp) reaction, where the proton in the final state arises due to the charge exchange of a proton in ^{3}He with a neutron in 1s or 1p shell in ^{12}C. Since the experimental data for the ^{12}C(^{3}He,t) reaction in the quasi-free region are of inclusive type, we do not include, in our calculations, the distortion potential for the proton in the final state. The main effect of distortion of the proton in the ^{12}C(^{3}He,tp) reaction is to remove the proton flux from this channel to other channels, which in the inclusive measurements is included in the data. Furthermore, since, due to strong absorption of the projectile and ejectile, the charge-exchange between the ^{3}He and ^{12}C nucleons occurs in the low density surface region of the nucleus, we consider the elementary process, pn→np, in the nucleus as a quasi-free process. In the present case, of course, this process is off-shell. We construct the t-matrix for it following our earlier studies on the elementary processes, p(n,p)n and p(p,Δ^{++})n [10]. In this work, the t-matrix is constructed in the DWBA, using one- pion plus rho-exchange potential for the $V_{\sigma\tau}$. This t- matrix reproduces the experimental data on the p(n,p)n reaction. For the p(p,Δ^{++})n reaction, incidentally, in the same work it was

found that only one-pion-exchange results agree with the experiments.

In section 2 we give the formalism for the (^{3}He,t) reaction. The transition amplitude is written in a distorted wave impulse approximation, as mentioned above, and distortions of ^{3}He and triton are treated in the eikonal approximation. We also present briefly the procedure to calculate the elementary t-matrix, $t_{\sigma\tau}$.

In the charge-exchange reaction, besides $t_{\sigma\tau}$, the cross-section also receives contribution from the iso-spin term, t_τ. Since, in Boson-exchange models, this t-matrix gets constructed from second- and higher-order Born terms only, we have not constructed it here. We have used for it the phenomenologically determined t-matrix of Franey and Love [11]. In any case, as we shall see later, the contribution of t_τ to the (^{3}He,t) cross-section is not much.

The experimental data for the ^{12}C(^{3}He,t) reaction, as obtained by Bergqvist et al. [3], exist for the triton energy spectrum at 2° to 7° emission angles at 2 GeV beam energy. These spectra are inclusive. The broad structure seen in them between 1.9 and 2 GeV triton energy can be ascribed to the quasi-free charge-exchange reaction. The theoretical cross-sections corresponding to these spectra are obtained by first calculating the double differential cross-section $d^2\sigma/dk_t dk_p$, and then integrating it over the allowed kinematics of the outgoing protons and summing over the various neutron states in the target nucleus. In section 3 we present the calculated differential cross-sections. The calculations are done with and without the ρ-exchange contribution in the interaction, and compared with the experimentally measured spectra. We find a reasonable overall agreement between the calculated and measured cross-sections with pi- plus rho-exchange interaction.

2 Formalism

The differential cross-section for the triton energy spectrum in the reaction ^{3}He + A $\rightarrow$t + p + B is given in the lab. as,

$$\frac{d^2\sigma}{dE_t d\Omega_t} = \int d(cos\theta_p) \times P \times \langle |T_{BA}|^2 \rangle, \qquad (1)$$

where $\langle |T_{BA}|^2 \rangle$ is the transition amplitude summed and averaged over the spins in the initial and final states respectively. The reaction mechanism is

shown in fig.1. k_{He} is taken along the z-axis and the x-z plane is defined by the vectors k_{He} and k_t. The factor P in the above eq. is given as,

$$P = \int \frac{d\phi_p}{2(2\pi)^5} \times \frac{k_t k_p^2 m_{He} m_t m_p m_B}{k_{He}[k_p(E_i - E_t) - k_{He} cos\theta_p E_p + k_t E_p cos(\theta_{pt})]}, \quad (2)$$

where E_x, k_x and m_x represent the energy, momentum and mass respectively of the particle x. θ_{pt} is the emission angle of the proton relative to the triton. For a given beam energy and fixed value of the triton four momentum, k_p is determined by solving the appropriate energy-momentum conservation relations. The cross-section $d^2\sigma/dE_t d\Omega_t$ is calculated by integrating over all possible emission directions, θ_p and ϕ_p, of the outgoing proton.

2.1 Evaluation of T_{BA}

The transition amplitude for the reaction A(^{3}He,t)B, in DWIA, is given as,

$$T_{BA} = (\chi^-_{\boldsymbol{k}_t}, k_p \langle B, t, p | \sum_{ij} [t_{\sigma\tau}(i,j) + t_\tau(i,j)] | A, ^3He \rangle \chi^+_{\boldsymbol{k}_{He}}), \quad (3)$$

where j represents the active nucleons in the target nucleus and i those in ^{3}He. χ_{He} and χ_t are the distorted waves for helium and triton respectively. For protons, because of the inclusive nature of the reaction, we use plane waves. This is appropriate, because, as discussed in the literature [12], the main effect of the distortion at intermediate energies is absorptive. This results in the transfer of flux from the given channel to other channels. In an inclusive reaction, these channels are included in the measured cross-sections.

$t_{\sigma\tau}(i,j)$ is the spin-isospin t-matrix, and contains the longitudinal and transverse components. It is off-shell. In terms of its central, t^C, and non-central, t^{NC}, components, we can write it as

$$t_{\sigma\tau}(i,j) = \left[t^C_{\sigma\tau}(\epsilon, q) \boldsymbol{\sigma}_i \cdot \boldsymbol{\sigma}_j + t^{NC}_{\sigma\tau}(\epsilon, q) S_{ij}(\hat{q}) \right] \boldsymbol{\tau}_i \cdot \boldsymbol{\tau}_j, \quad (4)$$

where $\mathbf{q}$ is the momentum transfer in the reaction and ϵ is the energy at which the elementary t-matrix for pn$\rightarrow$np needs to be evaluated. Actual evaluation of this t-matrix is described further below.

The tensor operator, $S_{ij}(\hat{q})$, is defined as :

$$S_{ij}(\hat{q}) = 3\sigma_i \cdot \hat{q}\sigma_j \cdot \hat{q} - \sigma_i \cdot \sigma_j$$
$$= [\frac{24\pi}{5}]^{1/2} \sum_M \sum_{\mu\nu} (-1)^{\mu+\nu} \sigma_\mu(i)\sigma_\nu(j)\langle 11-\mu-\nu|2M\rangle Y_{2M}(\hat{q}) \quad (5)$$

To evaluate T_{BA}, we first observe that, around the energy of interest of the continuum particles here ($\approx$2 GeV), the main effect of distortion is absorptive. The dispersive effects are small. Therefore, in evaluating the elementary t-matrix, $t_{\sigma\tau}$ (or t_τ), we approximate the momentum transfer, q, by that corresponding to the asymptotic momenta of ^{3}He and triton. The $\langle|T_{BA}|^2\rangle$ then factorizes as

$$\langle|T_{BA}|^2\rangle = \langle|G|^2\rangle|\rho(q)|^2, \quad (6)$$

where $\mathbf{q} = \mathbf{k}_{He} - \mathbf{k}_t$. $\rho(\mathbf{q})$ is the spatial ^{3}He$\rightarrow$t transition density factor and is normalized such that $\rho(0) = 3$. The factor $\langle|G|^2\rangle$, after taking the expectation value of the elementary t-matrix over the spin-isospin wave functions of ^{3}He and triton, and summing and averaging the square appropriately over the spin projections of ^{3}He and triton, works out as,

$$\langle|G|^2\rangle = \frac{4}{9}\frac{1}{(2J_B+1)} \sum_{m_p M_B} \Bigg[\sum_{m=-1}^{m=+1} [|t^C_{\sigma\tau}(\epsilon,q)F^{-m,+1}(Q)$$
$$+[\frac{24\pi}{5}]^{1/2} t^{NC}_{\sigma\tau}(\epsilon,q) \sum_{\nu M} (-1)^\nu \langle 11-m-\nu|2M\rangle Y_{2M}(\hat{q})F^{\nu,+1}(Q)|^2]$$
$$+|t_\tau(\epsilon,q)|^2|F^{+1}(Q)|^2\Bigg]. \quad (7)$$

Here, $\mathbf{Q} = \mathbf{k}_{He} - \mathbf{k}_t - \mathbf{k}_p$ is the momentum of the recoiling nucleus in lab. In the impulse approximation, this momentum equals (with opposite sign) to that of the struck neutron in the target nucleus. $F^{\mu,+1}(\mathbf{Q})$ is the 'distorted' Fourier transform of the spin-isospin overlap integral of the target and residual nucleus. In configuration space, it is given by,

$$F^{\mu,+1}(Q) = \langle B|\sum_i \chi^{-*}_{\boldsymbol{k}_t}(r_i)\chi^{-*}_{\boldsymbol{k}_p}(r_i)\chi^{+}_{\boldsymbol{k}_{He}}(r_i)\sigma_\mu(i)\tau_{+1}(i)|A\rangle$$
$$= \int dr\, \chi^{-*}_{\boldsymbol{k}_t}(r)\chi^{-*}_{\boldsymbol{k}_p}(r)\chi^{+}_{\boldsymbol{k}_{He}}(r)\phi^{BA}_{\mu,+1}(r), \quad (8)$$

where $\phi^{BA}_{\mu,+1}(\boldsymbol{r})$ is the overlap integral and is defined as

$$\phi^{BA}_{\mu,+1}(\boldsymbol{r}) = \langle B| \sum_i \delta(\boldsymbol{r} - \boldsymbol{r}_i)\sigma_\mu(i)\tau_{+1}|A\rangle. \tag{9}$$

For a shell model and a closed shell target nucleus (i.e. J_A=0), it is easy to work out this integral. In this case, for $F^{\mu,+1}(\mathbf{Q})$ we eventually get,

$$F^{\mu,+1}(Q) = \sqrt{6}\sum_{m_s}\sum_{lm_l}\langle l, 1/2, m_l, m_s|J_B, -M_B\rangle\langle 1, 1/2, \mu, m_s|1/2, m_p\rangle$$
$$\langle \chi^-_t \chi^-_p|\chi^+_{He}, \phi_{lm_l}\rangle. \tag{10}$$

For the purely isospin-dependent term, in a similar way, we obtain,

$$\frac{1}{(2J_B+1)}\sum_{M_B m_p}|F^{+1}(Q)|^2 = \sum_{l,m_l}\frac{1}{(2l+1)}|\langle \chi^-_t \chi^-_p|\chi^+_{He}\phi_{lm_l}\rangle|^2. \tag{11}$$

ϕ_{lm_l} in above eqs. is the spatial part of the wave function in nl shell of a neutron in the target nucleus. It is normalized such that, $\langle \phi_{lm_l}|\phi_{lm_l}\rangle = N_{nl}$, where N_{nl} is the number of neutrons in the shell.

In eq. (7) one may notice that the contributions of the spin-isospin dependent and the only isospin dependent part of the interaction to the cross-section enter incoherently. The central and non-central parts in the spin-isospin interaction, however, add coherently.

2.2 p(n,p)n t-matrix

For the construction of this t-matrix we follow our earlier work [10]. In this work, including the effect of elastic and other channels on $a \rightarrow b$ transition in nucleon-nucleon scattering, at intermediate energies we write

$$t_{ba}(\boldsymbol{k}_i, \boldsymbol{k}_f) = (\chi^{-*}_{\boldsymbol{k}_f}, \langle b|V_{\sigma\tau}|a\rangle, \chi^+_{\boldsymbol{k}_i}), \tag{12}$$

where χ's are the distorted waves for the pn relative motion. They are the solutions of potentials which describe the pn elastic scattering. Below the pion threshold, these potentials are available from boson- exchange models. However, in the energy region, which is of relevance in the present work and is above the pion threshold, these potentials need major modifications. In the absence of a reliable estimate of such modifications, we have used the

eikonal approximation (which is valid at higher energies) and have written χ's directly in terms of the elementary elastic scattering amplitude, f(k,q), as (for details see ref.[13]),

$$\chi_{\boldsymbol{k}}^{+}(\boldsymbol{r}) = e^{i\boldsymbol{k}\cdot\boldsymbol{r}}\left[1 + \frac{i}{k}\int_0^\infty qdqJ_o(qb)f(k,q)\right]. \tag{13}$$

Here the amplitude f(k,q) peaks at zero degree and falls off rapidly. Near the forward direction it can be reasonably parametrized as [14],

$$f(k,q) = f(k,0)exp(-\frac{1}{2}\alpha q^2), \tag{14}$$

where, using the optical theorem, we can further write,

$$f(k,q) = [\frac{k}{4\pi}]\sigma_T(k)(i+\beta(k))exp(-\alpha(k)q^2/2). \tag{15}$$

Here, σ_T is the total cross-section, β is the ratio of the real to imaginary part of the scattering amplitude and α is the slope parameter in the pn scattering. The values of these parameters depend upon the energy, k, of the pn system.

The t-matrix, with the above parametrization, works out to be

$$t_{ba}(\boldsymbol{k}_i,\boldsymbol{k}_f) = \int dr e^{i\boldsymbol{q}\cdot\boldsymbol{r}} exp[i\xi(b)]\langle b|V_{o\tau}|a\rangle, \tag{16}$$

where $\xi(b)$ is the phase-shift function, and is defined as

$$exp\Big[i\xi(b)\Big] = [1 - Cexp(-b^2/2\alpha)] + iC\beta exp(-b^2/2\alpha), \tag{17}$$

with $C = \sigma_T/4\pi\alpha$.

$V_{o\tau}$ is the spin-isospin dependent transition potential. The major portion of this interaction, as is well known [4], arises from the one-pion-plus rho-exchange potential. We, therefore, write

$$V_{o\tau}(i,j) = \Big[V_\pi(t)\boldsymbol{\sigma}_i\cdot\hat{q}\boldsymbol{\sigma}_j\cdot\hat{q} + V_\rho(t)(\boldsymbol{\sigma}_i\times\hat{q})\cdot(\boldsymbol{\sigma}_j\times\hat{q})\Big]\boldsymbol{\tau}_i\cdot\boldsymbol{\tau}_j, \tag{18}$$

where

$$V_x(t) = -\frac{f_x^2}{3m_x^2}F_x^2(t)\frac{q^2}{m_x^2 - t}. \tag{19}$$

$t = \omega^2 - \mathbf{q}^2$ is the four-momentum transfer. In the p(n,p)n reaction, however, this is same as the three momentum transfer squared. f_x is the xNN coupling constant, where x denotes π or ρ. $F_x(t)$ is the form factor at the xNN vertex. For it's form we use the monopole form, i.e.

$$F_x(t) = \frac{\Lambda_x^2 - m_x^2}{\Lambda_x^2 - t}, \tag{20}$$

where Λ is the length parameter.

Substituting eq.(18) in eq.(16) the central and non-central parts of the spin-isospin t-matrix, appearing in eqn. (7), work out as,

$$t^C_{\sigma\tau}(q) = \int e^{i\boldsymbol{q}\cdot\boldsymbol{r}} e^{i\xi(b)} V^C_{\sigma\tau}(r) d\boldsymbol{r}, \tag{21}$$

and

$$t^{NC}_{\sigma\tau}(q) Y_{2M}(\hat{q}) = \int e^{i\boldsymbol{q}\cdot\boldsymbol{r}} e^{i\xi(b)} V^{NC}_{\sigma\tau}(r) Y_{2M}(\hat{r}) d\boldsymbol{r}, \tag{22}$$

where, in terms of the pi- and rho-exchange potentials, in momentum space

$$V^C_{\sigma\tau}(t) = \frac{1}{3}[V_\pi(t) + 2V_\rho(t)], \tag{23}$$

and

$$V^{NC}_{\sigma\tau}(t) = \frac{1}{3}[V_\pi(t) - V_\rho(t)]. \tag{24}$$

A detailed presentation of the above t-matrix for the elementary charge-exchange reaction and its applicability to the available experimental data over a wide energy range is being reported separately.

3 Results and Discussions

We calculate the double-differential cross-sections for the triton energy spectrum at a helium beam energy of 2 GeV and triton emission angles of 2^o to 7^o. Within the framework of the formalism given in the preceding sections, various inputs, which determine these cross-sections, are : (i) ϕ_{nl}, the radial wave function of the neutron in the target nucleus. (ii) ^{3}He$\rightarrow$t, transition form factor, $\rho(q)$. (iii) Parameters associated with the one-pion- and rho-exchange potentials. (iv) Parameters of the elastic pn scattering amplitude, f(k,q), and (v) ^{3}He and triton distorted waves.

The single particle wave functions, ϕ_{nl}, are generated in a Woods-Saxon potential, whose parameters are fixed from the analyses of the electron scattering and (p,2p) data on ^{12}C [15]. The neutron binding energies in the $1s_{1/2}$ and $1p_{3/2}$ orbitals in ^{12}C are taken equal to 34 MeV and 16 MeV respectively.

For the ^{3}He$\rightarrow$t transition form factor, $\rho(q)$, following the work of Dmitriev et al. [16], we use,

$$\rho(q) = F_o\, e^{-\gamma q^2}[1 + \eta q^4], \tag{25}$$

where $F_o = 0.96$, γ= 11.15 GeV^{-2} and η= 14 GeV^{-4}. This form factor has been obtained using (s+d) wave mixed wave functions for ^{3}He and triton. The second term in the square brackets in the above eqn. is related to the d-wave admixture. This form factor is found to be good upto large momentum transfers.

For the various parameters in the pion- and rho-exchange potentials, we use $f_\pi = 1.008$, $f_\rho = 7.815$, $\Lambda_\pi = 1.2$ GeV/c and Λ_ρ= 2 GeV/c. These values are consistent with several experimental observations, like, πN scattering, NN scattering [17], electro-disintegration of the deuteron [18], deuteron properties [19] and dispersive theoretical approaches [20]. In the value of f_ρ, of course, there is some uncertainty. It is 4.83, as determined by the vector dominance model [21], and is 7.815 as determined from the nucleon form factor and nuclear phenomena [22].

The elastic pn scattering amplitude, f(k,q), has three parameters: the total cross-section, σ_T, the slope parameter, α, which determines it's momentum transfer (q) behaviour, and the parameter, β, which determines the ratio of the real to imaginary parts of f(k,q). Except β, both other parameters are well known from the measured experimental data on the pn scattering [23]. The energy, k, at which these parameters need to be taken is, of course, not defined well. This happens because of the Fermi motion of the nucleons in the projectile and the target nuclei. However, as the beam energy is high, for the purpose of fixing the values of these parameters, we ignore the Fermi motion of the proton in the beam and the struck neutron in the target. The energy of pn system in lab., therefore, is taken equal to 1/3 of the ^{3}He energy. Corresponding to 2 GeV ^{3}He energy, we find $\alpha \approx 6$ (GeV/c)$^{-2}$ and $\sigma_T \approx$34 mb. In the value of β, there exists lot of uncertainty in the 'measured' values [24]. At the energy of our interest, it ranges from 0.05 to -0.7. We have

chosen the value -0.45 for our purpose. The calculated cross-sections with this value of β are found in most reasonable agreement with the experimental data. We will, of course, exhibit later the sensitivity of our results to the value of β.

For the only iso-spin dependent part of the t-matrix, t_τ, we use the phenomenologically determined t-matrix of Franey and Love [11] from NN scattering experiments at 725 MeV beam energy. The contribution of this term to the cross-section, however, as we shall see later, is not much.

The distorted waves for helium and triton appear as a product in eqs. (10,11). In the eikonal approximation, this can be approximated as follows,

$$\chi_t^{-*}\chi_{He}^{+} = e^{iq_\parallel z}\, e^{i\boldsymbol{q}_\perp\cdot\boldsymbol{b}} e^{2i\delta(b)}, \tag{26}$$

if we ignore the difference between the phase shifts of ^{3}He and triton (around 2 GeV). Here $\delta(b)$ corresponds to the phase shift of a mass 3 particle. The phase shift function $\delta(b)$ can be constructed, in principle, from optical potentials. But, since this is a poorly known quantity, we refer to the experimentally measured values. The experimental $\delta(b)$ too is not available for mass 3 particles and hence we use the phase shifts obtained from alpha scattering at 1.37 GeV on calcium isotopes [25]. Here, $exp[2i\delta(b)]$, which gives a good description of the α scattering data, is found to be purely real and has a 1 minus Woods-Saxon form. The radius parameter $r_o(R = r_o A^{1/3})$, and diffuseness, a, of this functional form are found equal to 1.45 and 0.68 fm. respectively. We use this phase shift function for our purpose too, except that the radius, R, is put corresponding to A=12.

Before we present the calculated cross-sections, in fig. 2 we show at 2 GeV beam energy the range of momentum transfer (q) involved in the triton emission upto 7^0 in lab. In the quasi-elastic range of the triton energy (i.e. upto 1900 MeV), this momentum transfer, as we see, is not small. At 2-3 degree it is around 250 MeV/c, and at larger angles it goes to about 500 MeV/c. This suggests that the non-central component of the t-matrix, T_{BA}, and hence the ρ-exchange part of the $V_{\sigma\tau}$ (whose contribution increases at larger q), may effect the quasi-elastic cross-section significantly. However, because the rho-exchange contributes with opposite signs to the central and non-central pieces of the potential (see eqs. 23, 24), it is not immediately obvious as how much, in net, the rho-exchange would change the cross-sections. In fig. 3 we plot the typical central and non-central components of the real

part of the calculated elementary t-matrix used in our calculations. We show this t-matrix for a pure one-pion-exchange potential and for a one pion- plus rho-exchange potential. As expected, we see that the rho-exchange affects both the pieces of the t-matrix significantly, but in the opposite directions.

To demonstrate the extent to which the above t-matrix reproduces the measured p(n,p)n cross-sections, in fig. 4 we show the calculated 0^0 cross-sections alongwith the experimental data [26-33] over a large energy range. As we see, the calculated cross-sections are in good accord with the measured cross-sections.

In fig. 5 we show the results for the $^{12}C(^3He,t)$ reaction together at all the angles of the triton emission. In fig. 5a we see a representation of the experimentally measured cross-sections and in fig. 5b that of our corresponding theoretically calculated results. The calculated cross-sections are obtained with the pion and rho meson both included, and with contributions from the spin-flip and non-spin-flip channels to the transition matrix. As can be seen from the figs., the overall behaviour of the experimental cross-sections, which includes the magnitude and position of the peak and its shift with the emission angle of the triton, gets reproduced reasonably well by the theoretical calculations. This vindicates, in essence, the applicability of the quasi-free mechanism framework presented in the earlier section to the region of the triton spectrum lying between the bound nuclear states and the delta production region.

In the following, we give the results at each angle separately.

In figs. 6, 7 and 8 we show the triton energy spectra plotted individually for six triton emission angles between 2^o and 7^o. The solid curves represent the calculations with the one-pion plus one-rho exchange interaction. The experimental results are represented by the dots. Except at 5^o and 7^o, we find a good accord between the calculated and measured cross- sections. The underestimation of the cross-sections at 7^o should not be a source of much discouragement, as the magnitude of the cross-section is too small at this angle ($\sim 7\mu b$). Therefore, the measured cross-section can have large uncertainty and a significant contribution from other reaction mechanisms. The reason for the overestimation of the cross-section by about a factor of 3/2 at 5^0 is, of course, not clear to us.

To isolate the contribution due to rho-exchange to the calculated cross-sections, in figs. 6-8 we also display, by dashed curves, the cross-sections with only the one-pion-exchange transition potential. As we see from these

figs., the contribution of the rho-exchange changes continuously from being positive at 2° to negative at 7°. Around 3^0 it crosses the zero level. This happens, as mentioned earlier, due to change in the momentum transfer, q, (see fig. 2) and the opposite signs of the rho-exchange potential in the central and the non-central pieces of the potential. At smaller momenta, where the central term dominates, the rho-exchange comes with the positive sign, while at larger angles, where the non-central term is important, it comes with the negative sign (see eqs. 23, 24 and fig. 3).

In our calculations, we also find that the calculated cross-sections are mainly decided by the spin-isospin dependent part of the t-matrix. This can be seen in fig. 9, where we show the 2^0 calculated cross-sections with and without the isospin-dependent term, t_τ. The dashed curve represents the calculation without the isospin-dependent term in the t-matrix, while the solid curve is the complete calculation. As we see, the only isospin-dependent term makes a contribution of less than 10% to the cross-section.

As we mentioned earlier, the only uncertain parameter in the above calculations had been the value of the parameter β - the ratio of the real to imaginary part of the elementary scattering amplitude. In fig. 10 we show the calculated triton energy spectrum at 2^0 and 6^0 for three values of β, viz. 0.05, -0.45 and -0.7. These values lie within the uncertainty of the experimentally extracted value. As we see, the calculated cross-sections do depend upon the value of β. For the present range, it can change the peak cross-section by a factor of 2.

The quasi-free cross-sections, as we see from the examination of the expression (eqs. 6,7) for $\langle|T_{BA}|^2\rangle$, is essentially determined by, (i) the t-matrix, $t_{\sigma\tau}$, and (ii) the neutron momentum distribution in the target nucleus through the recoil momentum distribution factors, $F^{\nu,+1}(\mathbf{Q})$ and $F^{+1}(\mathbf{Q})$. The $t_{\sigma\tau}$ depends upon q, and F's on Q. In fig. 2 we see that the magnitude of q, at a particular triton emission angle, does not vary much in the region of the quasi-elastic peak. This means that the elementary t-matrix, $t_{\sigma\tau}$, too does not change much over this region for a fixed triton emission angle. Consequently, in the A(^{3}He,t)B reaction, the elementary t-matrix mainly affects the magnitude of the cross-sections (see e.g. fig. 10). The shapes of the triton energy spectra, which in the inclusive data mean the peak position and the width, are decided by the the recoil momentum distribution factors. Since in the inclusive data the proton in the final state is not detected, and $\mathbf{Q} = \mathbf{k}_{He} - \mathbf{k}_t - \mathbf{k}_p$, each point in the triton energy spectrum involves an

integral over a certain range of Q. This means that even the shape of the triton energy spectra might not depend upon the details of the neutron momentum distribution in the nucleus. It may be sufficient if the neutron wave functions have correct separation energies for different shells and reproduce some gross properties, like the r.m.s. radius, of the nucleus. To exhibit this, in fig. 11 we show the calculated cross-sections for two radial wave functions, ϕ_{nl}, of the neutron in the target nucleus. The solid curve is the calculation with ϕ_{nl} generated in a Woods-Saxon potential as has been used through out this work; the dashed curve is the calculation using harmonic oscillator wave function with the oscillator parameter b=1.66 fm, which is consistent with the electron scattering data. As can be seen from the figure, within about 10%, the two results are same.

4 Conclusions

We have examined the quasi-elastic peak region in the ^{12}C(^{3}He,t) reaction at 2 GeV over a range of triton emission angles from 2° to 7°. We have calculated the triton energy spectra in the framework of a quasi-elastic charge-exchange between a proton in the projectile and a neutron in the target nucleus. Constructing the t-matrix for this process with the $\pi + \rho$ transition potential, and using distorted waves for ^{3}He and triton, the overall features of the experimentally measured cross-sections are produced reasonably well. Various inputs used for these calculations are constrained by other known experimental quantities, and thus are not arbitrary.

5 Acknowledgements

One of the authors (N.G.K.) wishes to thank the support given by the Department of Atomic Energy, Government of India, for part of the work which was done at the Bhabha Atomic Research Centre in Bombay.

References

[1] G. Jacob and A. J. Maris, Nucl. Phys. **31**, 139 (1962); *ibid* Rev. of Mod. Phys. **38**, 121 (1966); T. Berggren and H. Tyren, Ann. Rev. Nucl. Sci. **16** , 153 (1966); D. F. Jackson, Adv. Nucl. Phys. **4**, 1 (1971); R. E. Chrien *et al.*, Phys. Rev. **C21**, 1014 (1980); J. S. O'Connell *et al.*, Phy. Rev. **C35**, 1063 (1987).

[2] B. E. Bonner *et al.*, Phy. Rev. **C18**, 1418 (1978); C. Gaarde, Nucl. Phys. **A507**, 79c (1990).

[3] I. Bergqvist *et al.*, Nucl. Phys. **A469**, 648 (1987);

[4] G. E. Brown, J. Speth and J. Wambach, Phy. Rev. Lett. **46** , 1057 (1981).

[5] W. M. Alberico, M. Ericson and A. Molinari, Phys. Lett. **92B**, 153 (1980); *ibid* Nucl. Phys. **A379**, 429 (1982);

[6] D. M. Contardo *et al.*, Phys. Lett. **168B**, 331 (1986); C. Ellegard *et al.*, Phys. Rev. Lett. **50**, 1745 (1983); *ibid* Phys. Lett. **154B**, 110 (1985); D. Bachelier *et al.*, Phys. Lett. **172B**, 23 (1986).

[7] W. M. Alberico *et al.*, Phys. Rev. **C38**, 109 (1988).

[8] M. Ichimura *et al.*, Phys. Rev. **C39**, 1446 (1989).

[9] G. F. Bertsch, L. Frankfurt and M. Strkman, Science **259**, 773 (1993).

[10] B. K. Jain and A. B. Santra, Phys. Rev. **C46**, 1183 (1992); *ibid* Phys. Rep. **230**, 1 (1993).

[11] W. G. Love and M. A. Franey, Phy. Rev. **C24**, 1073 (1981); M. A. Franey and W. G. Love, Phys. Rev. **C31**, 488 (1985);

[12] N. Austern and C. M. Vincent, Phys. Rev. **C23**, 1847 (1981).

[13] B. K. Jain and A. B. Santra, Nucl. Phys. **A519**, 697 (1990); *ibid* Phy. Lett. **B244**, 5 (1990).

[14] H. Palevsky *et al.*, Phys. Rev. Lett. **18**, 1200 (1967); G. J. Igo *et al.*, Nucl. Phys. **B3**, 181 (1967); B. A. Ryan *et al.*, Phys. Rev. **D3**, 1 (1971).

[15] L. R. B. Elton and A. Swift, Nucl. Phys. **A94**, 52 (1967); R. Shanta and B. K. Jain, Nucl. Phys. **A175**, 417 (1971).

[16] V. F. Dmitriev, O. Sushkov, and C. Gaarde, Nucl. Phys. **A459**, 503 (1986).

[17] R. Machleidt, K. Holinde and C. Elester, Phys. Rep. **149**, 1 (1987); W. N. Cottingham *et al.*, Phys. Rev. **D8**, 800 (1973).

[18] J. F. Mathiot, Nucl. Phys. **A412**, 201 (1984).

[19] T. E. O. Ericson and M. Rosa-Clot, Nucl. Phys. **A405**, 497 (1983).

[20] W. Nutt and B. Loiseau, Nucl. Phys. **B104**, 333 (1976).

[21] M. M. Nagels *et al.*, Nucl. Phys. **B109**, 1 (1976).

[22] G. Hohler and E. Pietarinen, Nucl. Phys. **B95**, 210 (1975).

[23] B. H. Silverman *et al.*, Nucl. Phys. **A499**, 763 (1989).

[24] W. Grein, Nucl. Phys. **B131**, 255 (1977).

[25] D. C. Choudhury, Phys. Rev. **C22**, 1848 (1980).

[26] P. F. Shepard, T. J. Devlin, R. E. Mischke and J. Solomon, Phys. Rev. **D10**, 2735 (1974); R. E. Mischke, P.F. Shepard and T.J. Devlin, Phy. Rev. Lett. **23**, 542 (1969).

[27] B. E. Bonner *et al.*, Phy. Rev. Lett. **41**, 1200 (1978).

[28] W. Hurster *et al.*, Phys. Lett. **B90**, 367 (1980).

[29] G. Bizard *et al.*, Nucl. Phys. **B85**, 14 (1975).

[30] Yu. M. Kazarinov and Yu. N. Simonov, Zh. Eskp. Teor. Fiz. **43**, 35 (1962) (Sov. Phys. JETP **16**, 24 (1963)).

[31] V. J. Howard *et al.*, Nucl. Phys. **A218**, 140 (1974).

[32] D. F. Measday, Phy. Rev. **142**, 584 (1966).

[33] J. N. Palmieri and J.P. Wolfe, Phy. Rev **C3**, 144 (1971).

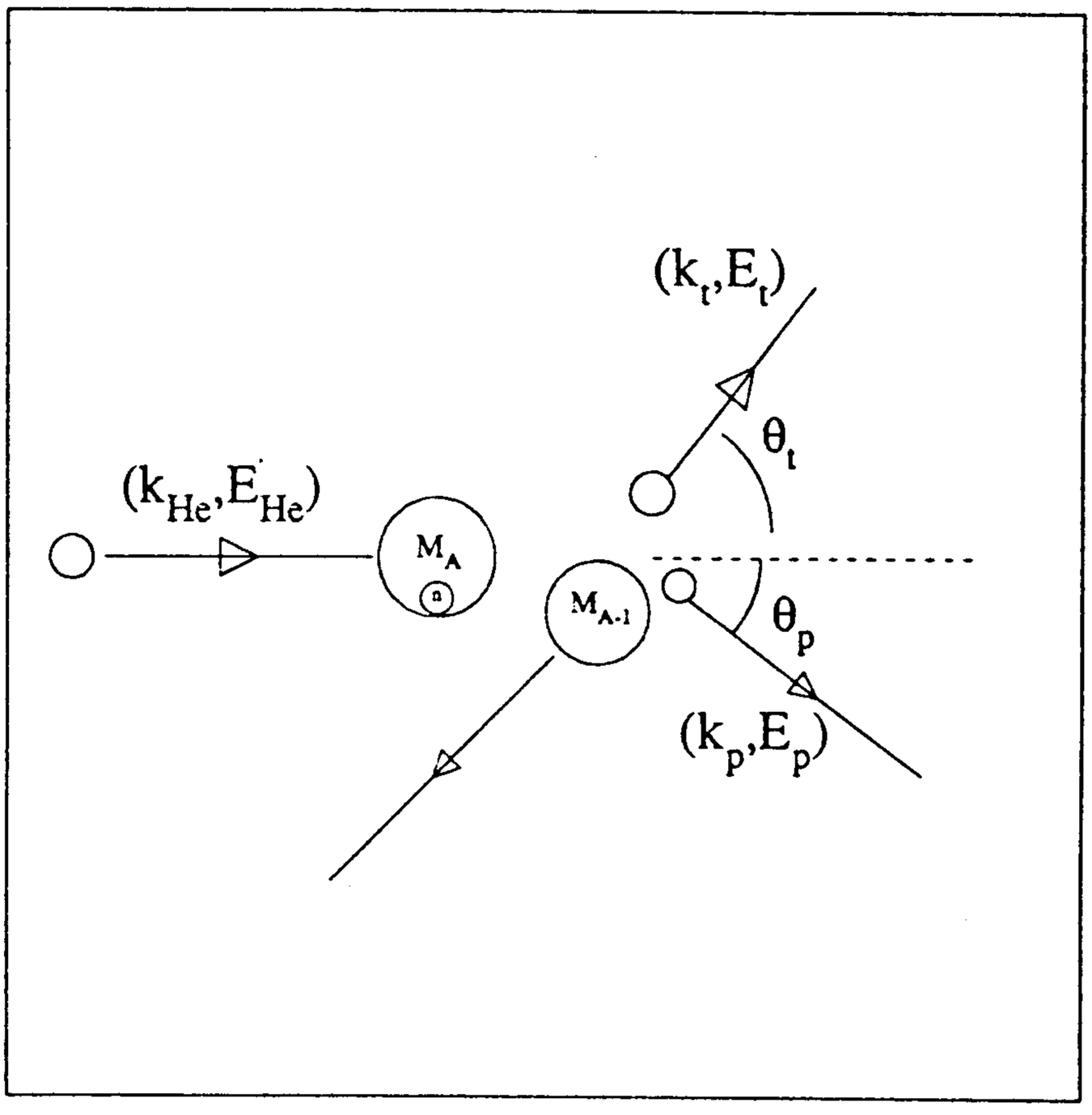

Fig. 1

Diagrammatic representation of the reaction $^3He + {}^{12}C \rightarrow t + p + {}^{11}C$.

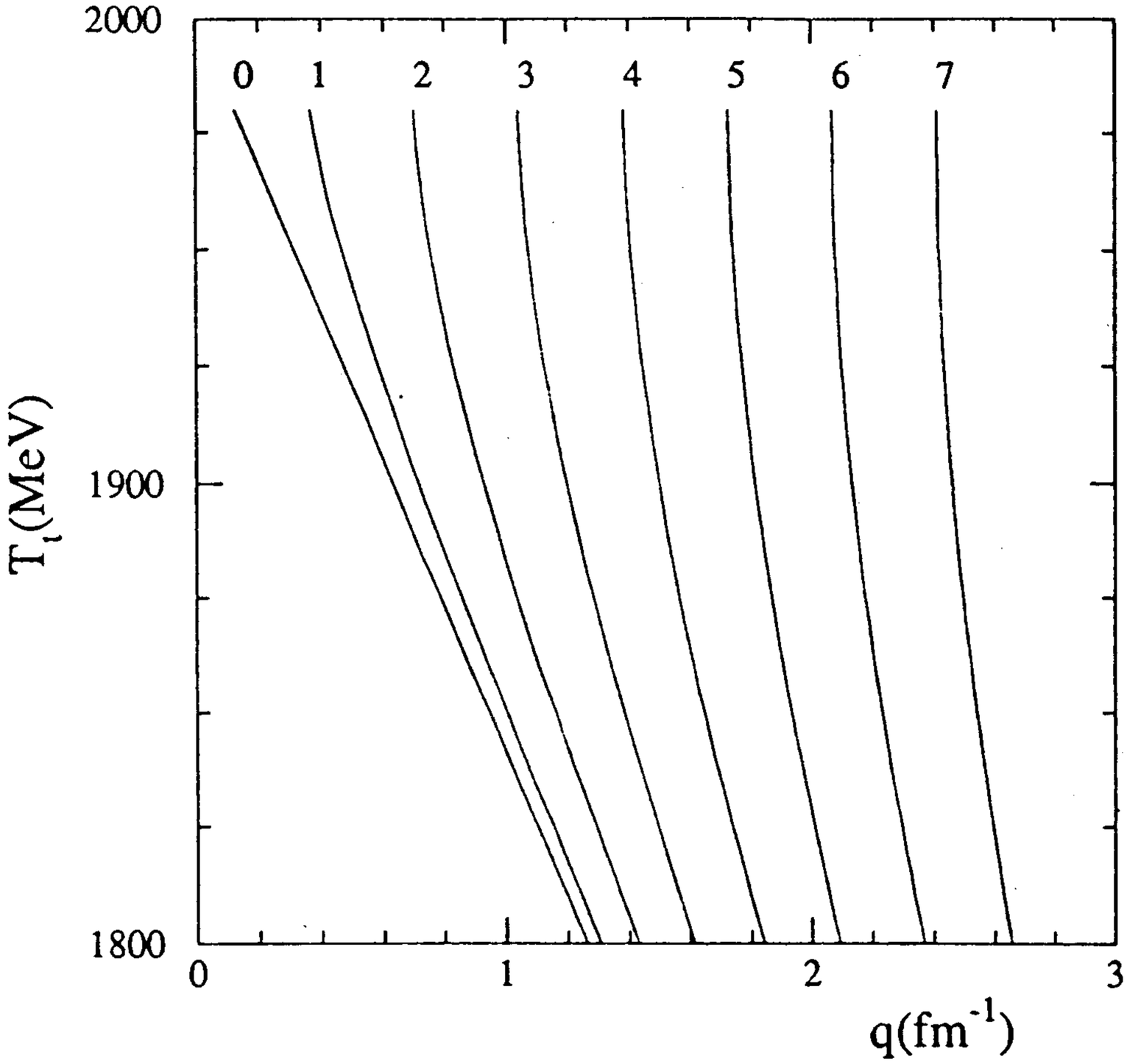

Fig. 2

Kinematics for the $^{12}C(^3He,t)$ reaction at $T_{He} = 2$ GeV. The triton energies are plotted as a function of the momentum transfer q, for triton emission angles of 0° to 7°.

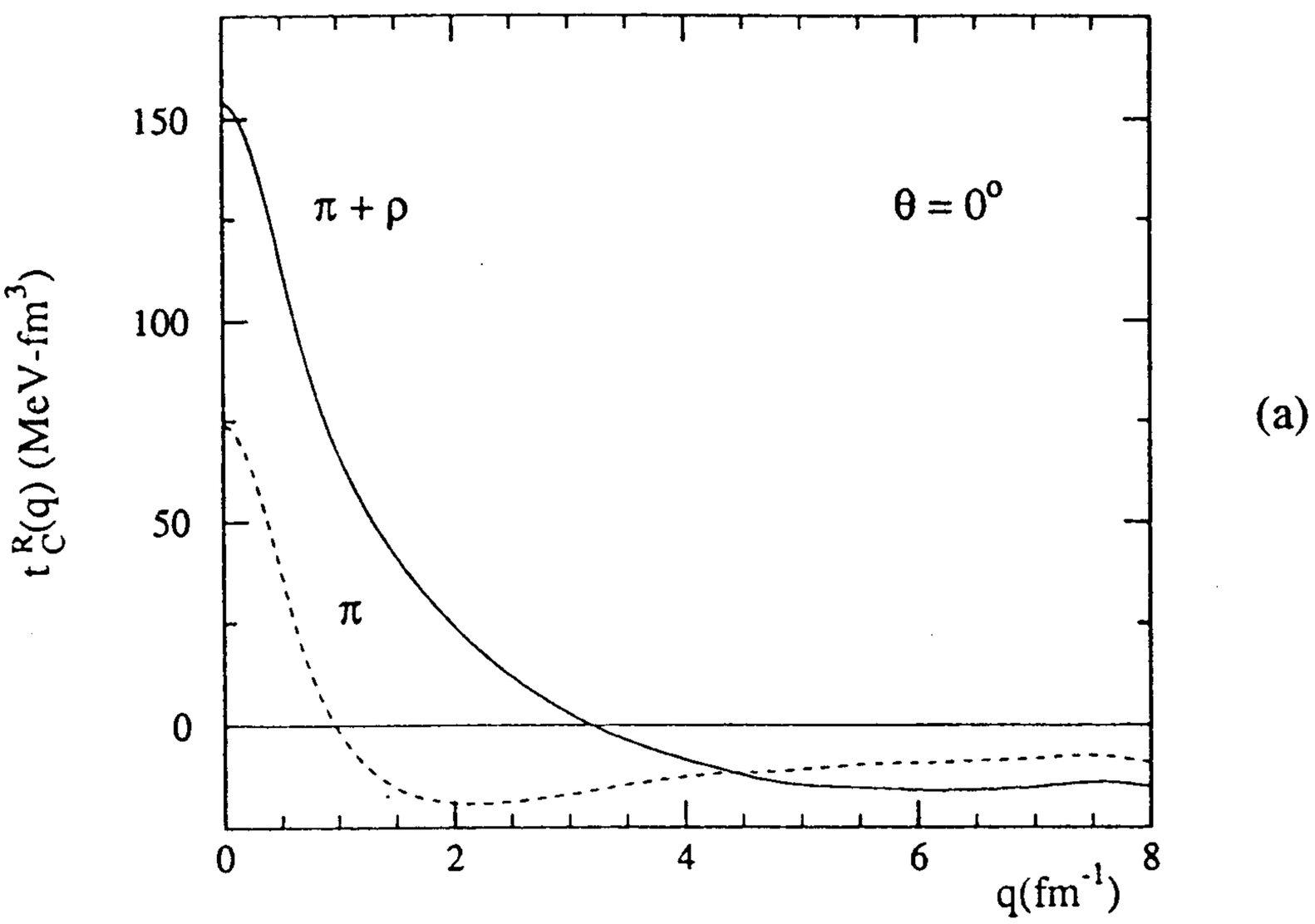

(a)

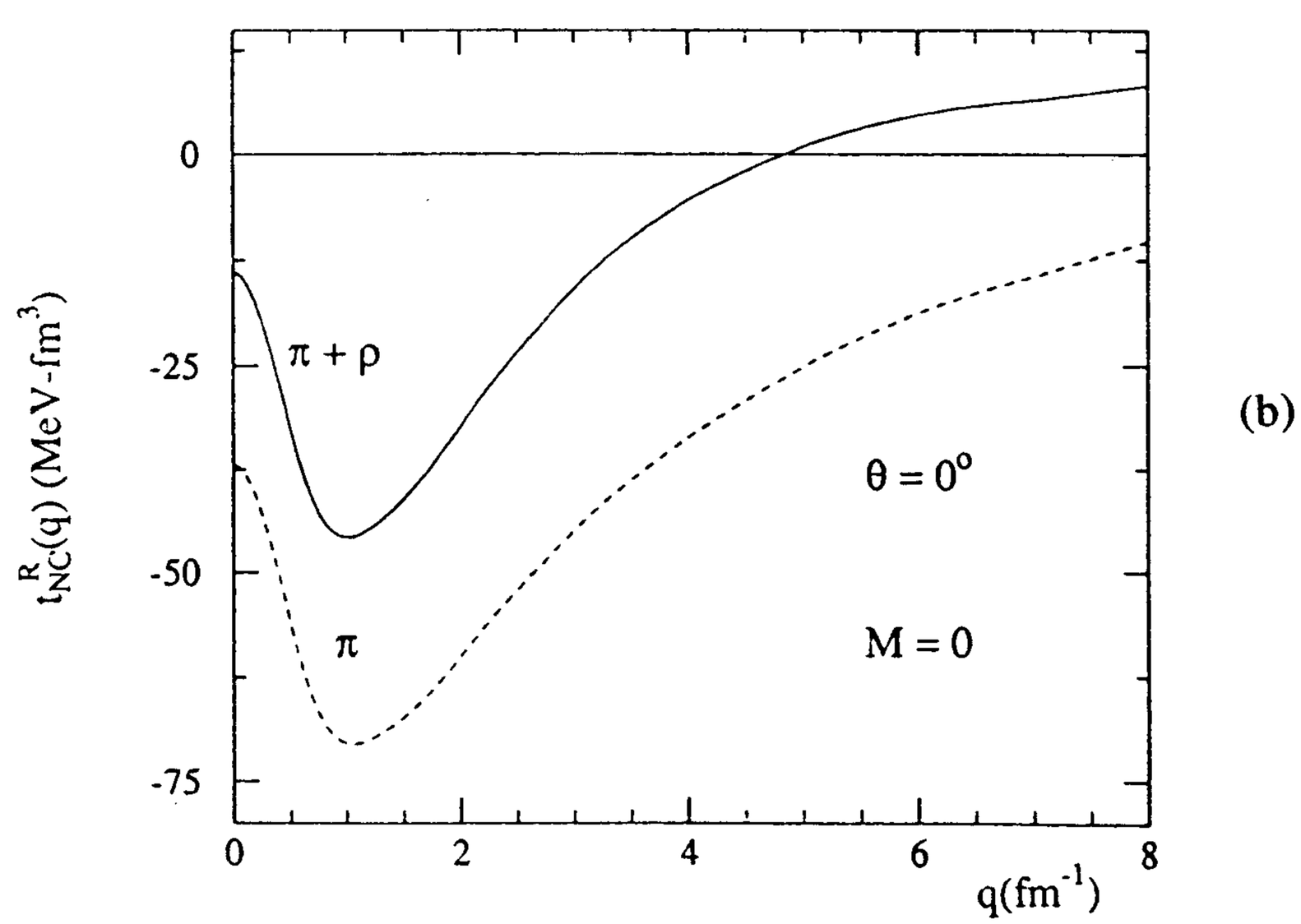

(b)

Fig. 3

Real part of the t-matrix as a function of the momentum transfer $\mathbf{q} = \mathbf{k}_{He} - \mathbf{k}_t$. Solid curves represent the t-matrix constructed with the $\pi + \rho$ exchange transition potential and dashed curves the one-pion exchange only. (a) Central part of the t-matrix (b) Non-central part of the t-matrix.

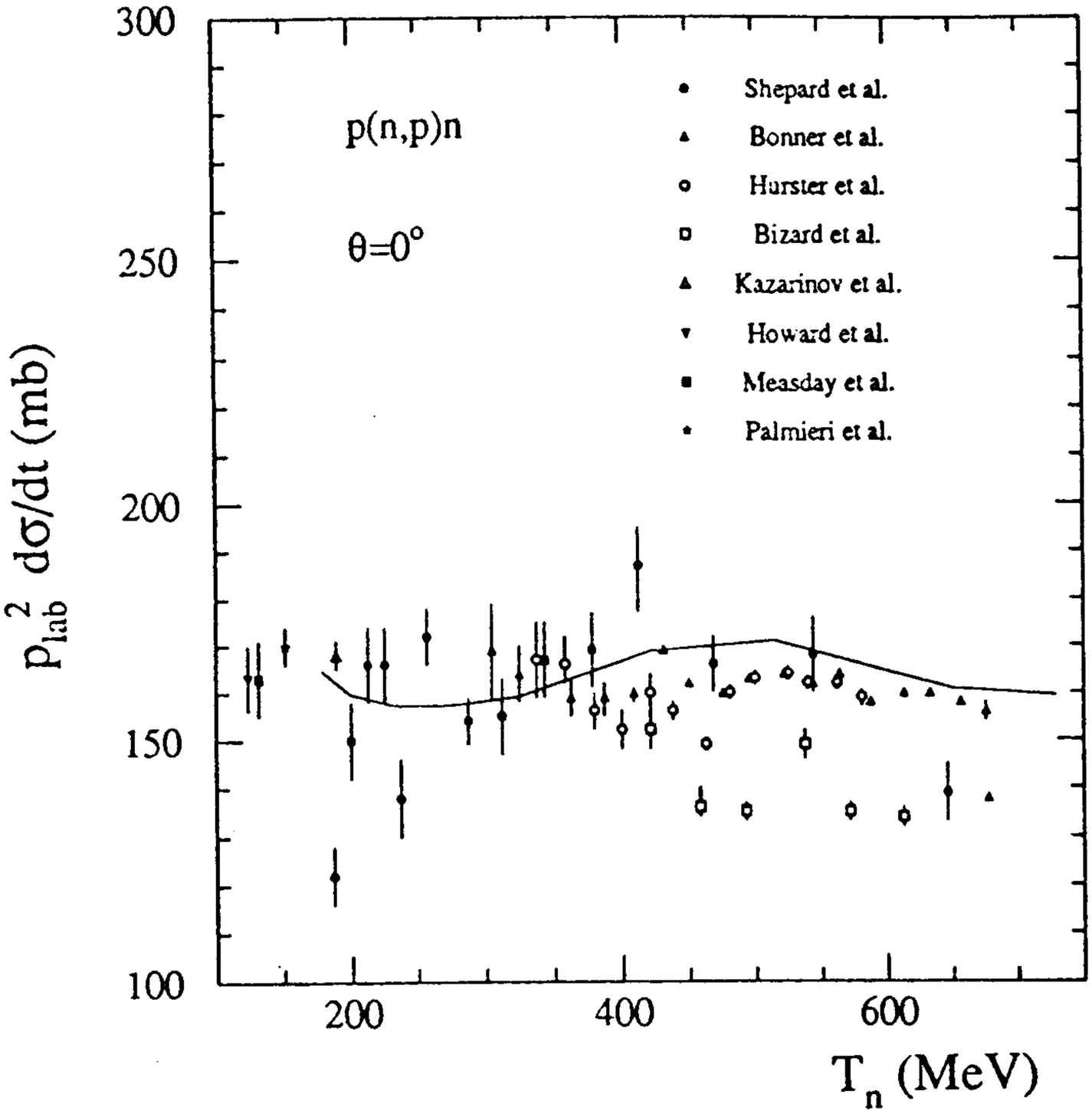

Fig. 4

Calculated and measured p(n,p)n cross-sections at 0^0 for various neutron energies. The calculated cross-sections are for one pion- plus rho-exchange spin-isospin potential.

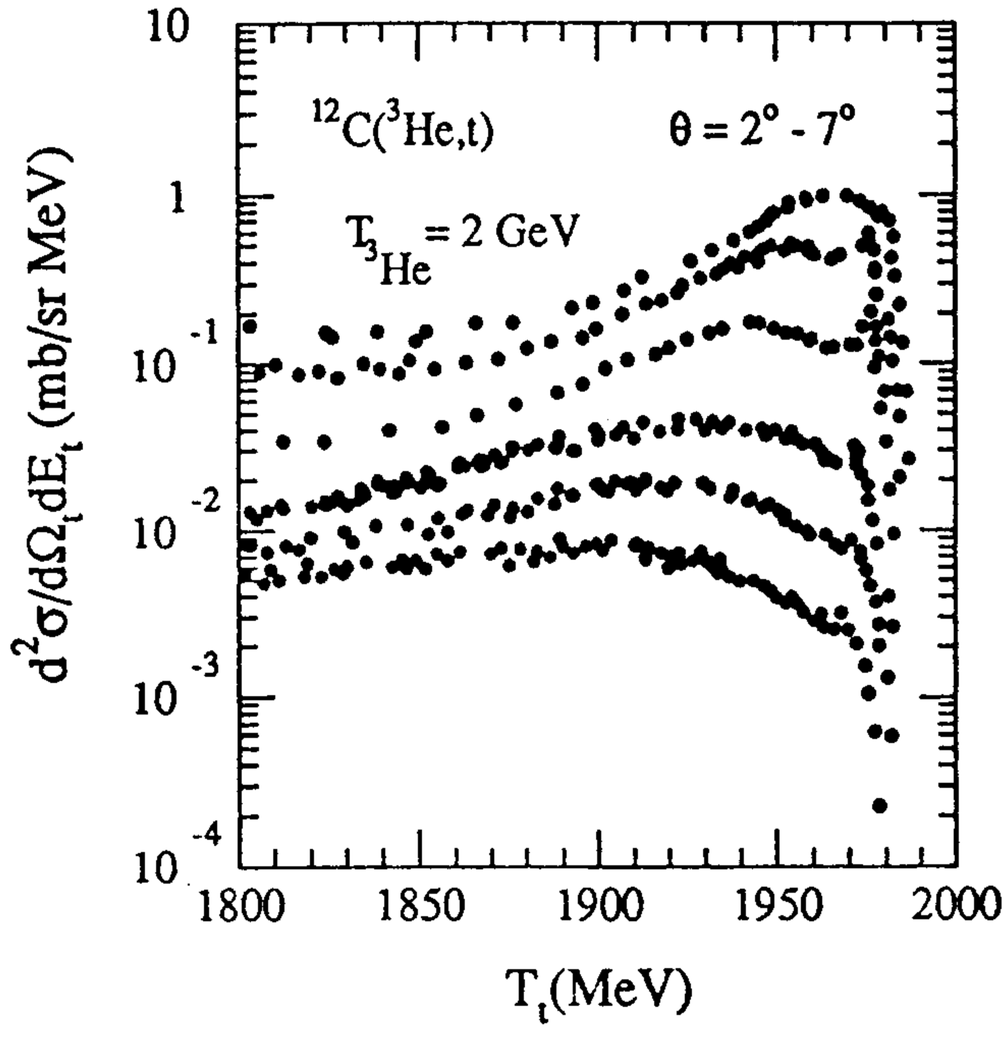

(a)

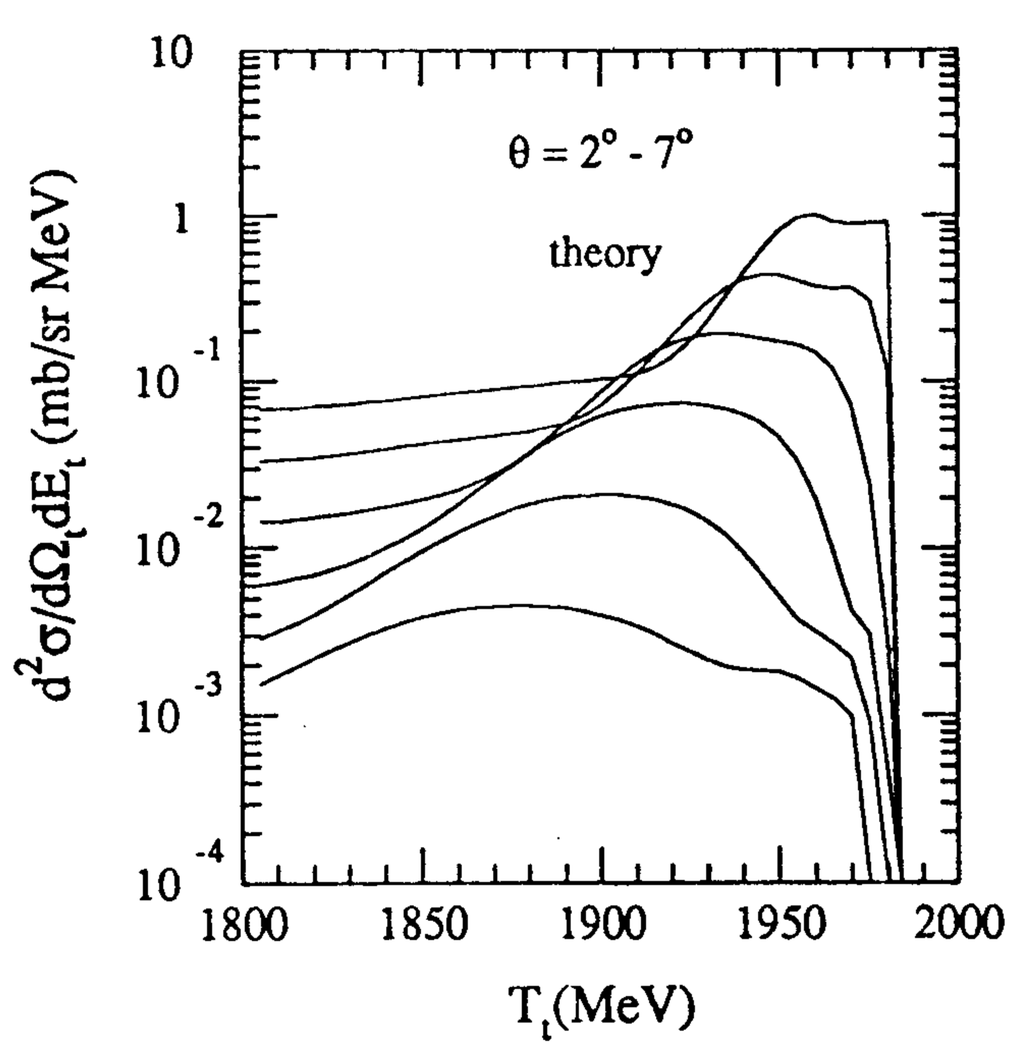

(b)

Fig. 5

Triton energy spectra in the quasi-elastic peak region for $^{12}C(^3He,t)$ at incident beam energy $T_{He} = 2$ GeV and triton emission angles of 2^o to 7^o. (a) Representation of the experimental data from ref.[3]. (b) Theoretical calculations with the $\pi + \rho$ exchange transition potential.

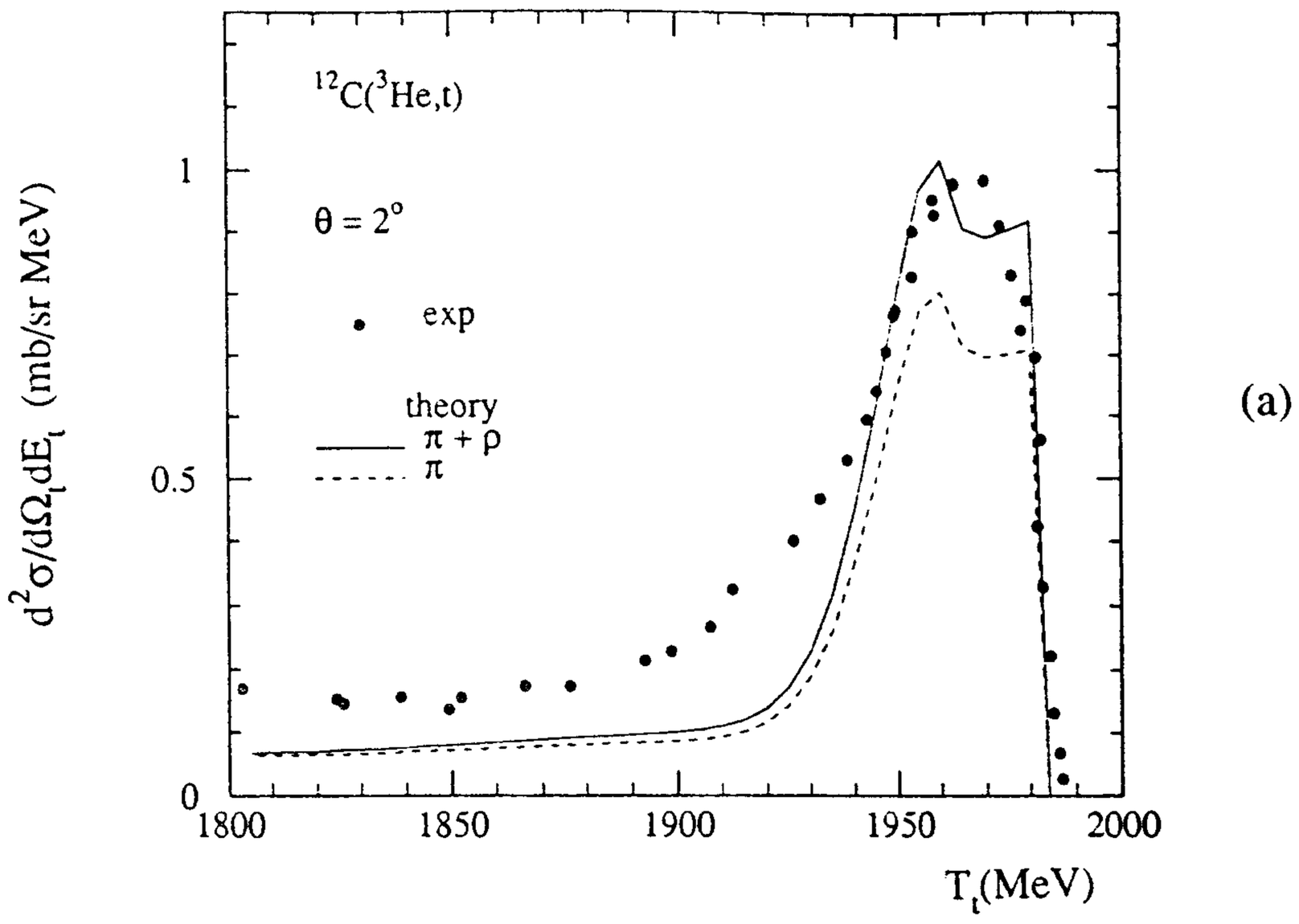

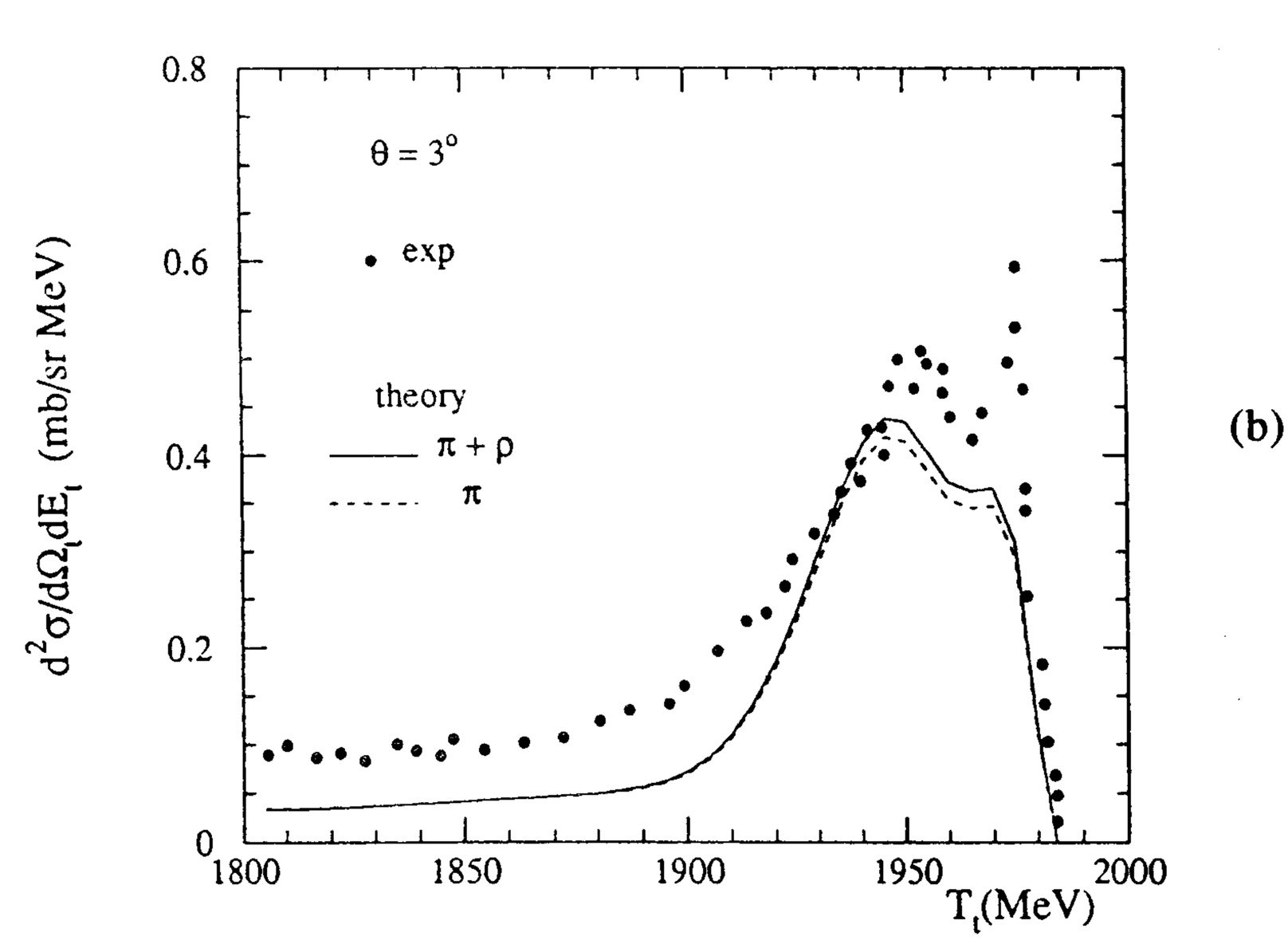

Fig. 6 ·

Triton energy spectra in the quasielastic peak region at triton angles of 2^o and 3^o for $^{12}C(^3He,t)$ at 2 GeV beam energy. The solid curves are the cross-sections with the t-matrix consisting of the $\pi + \rho$ exchange transition potential. The dashed curves are the results with only one-pion exchange. Dots represent the experimental data (ref.[3]).

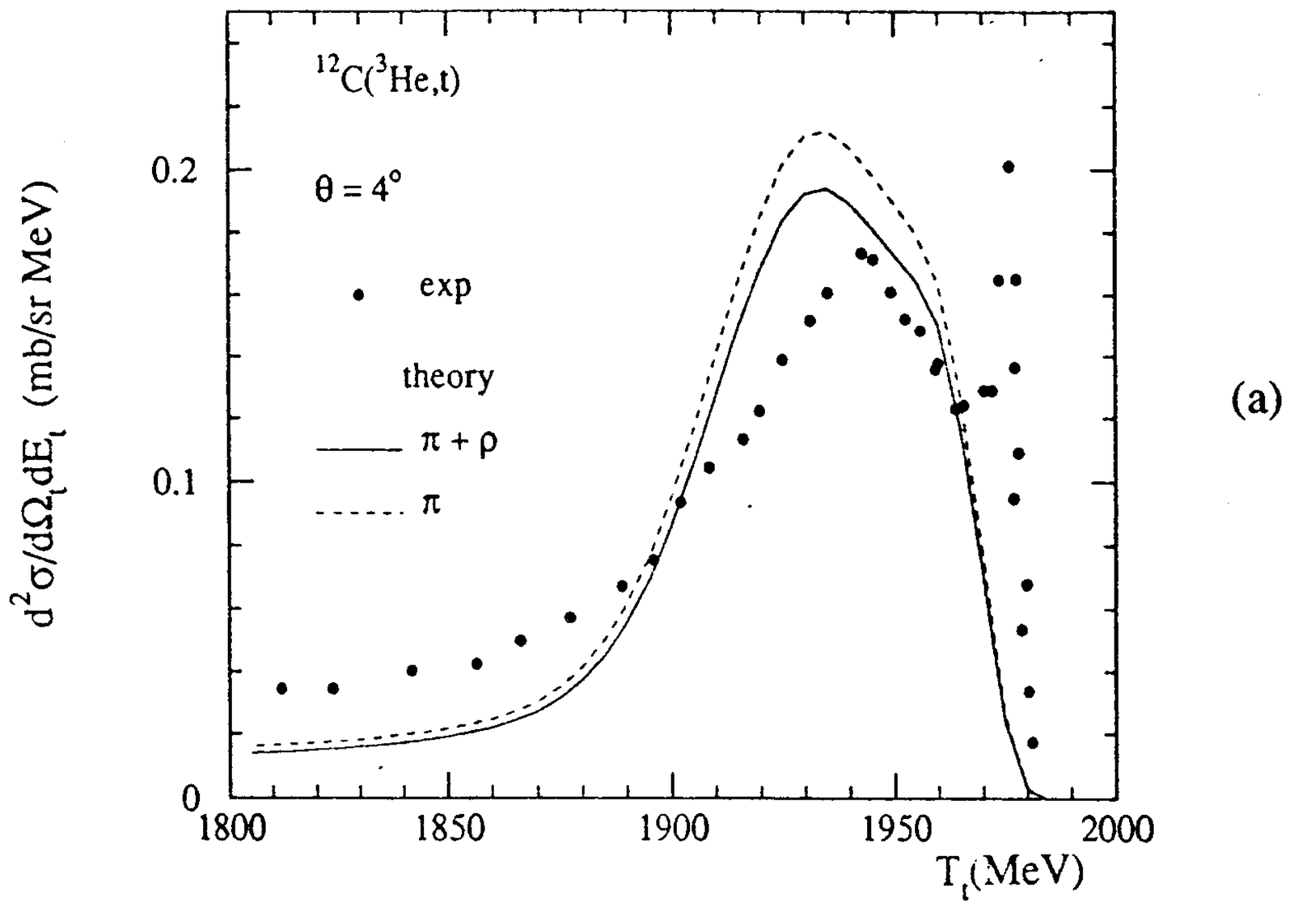

Fig. 7

Same as fig. 6 for triton emission angles of 4° and 5°.

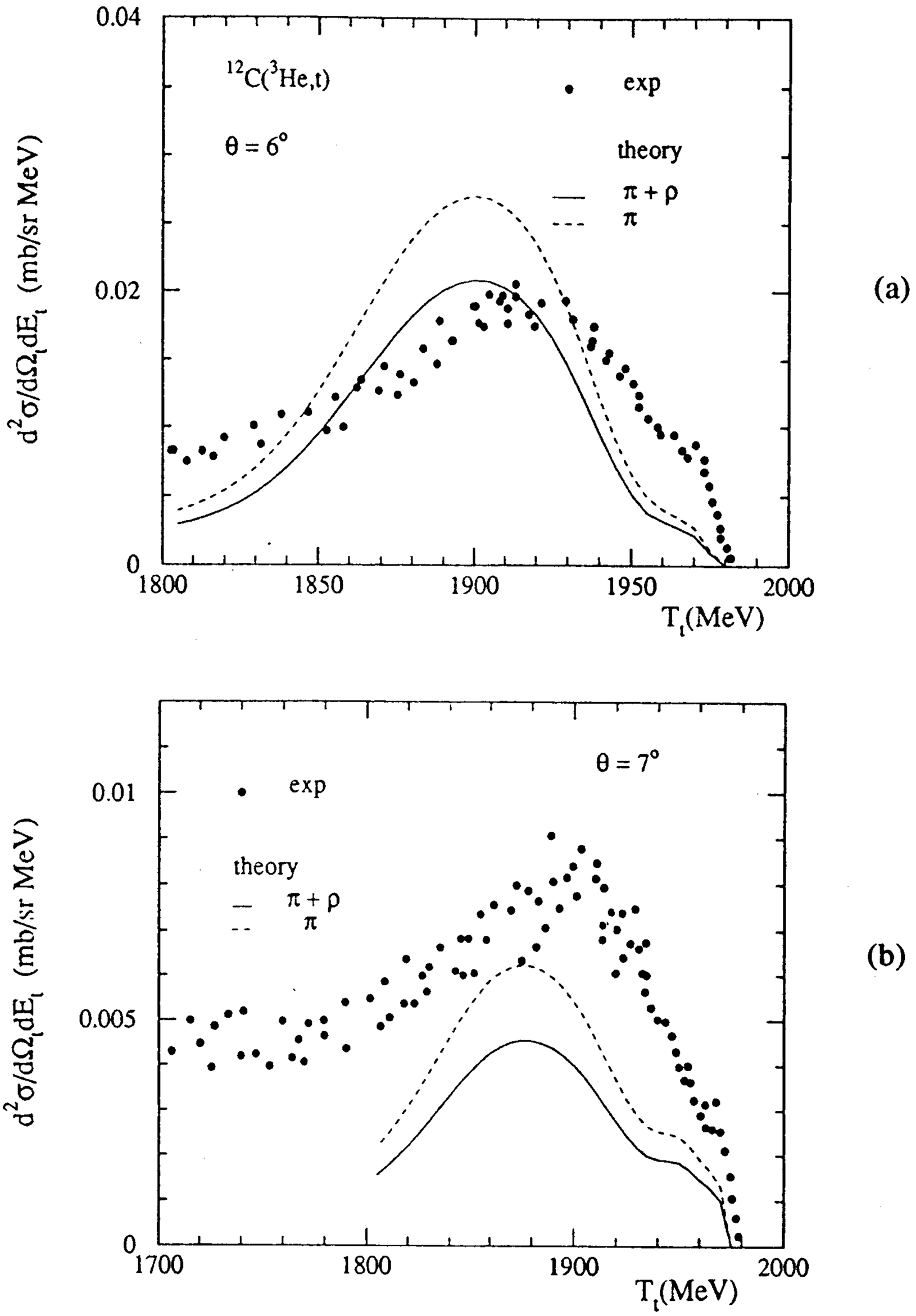

Fig. 8

Same as fig. 6 for triton emission angles of 6° and 7°.

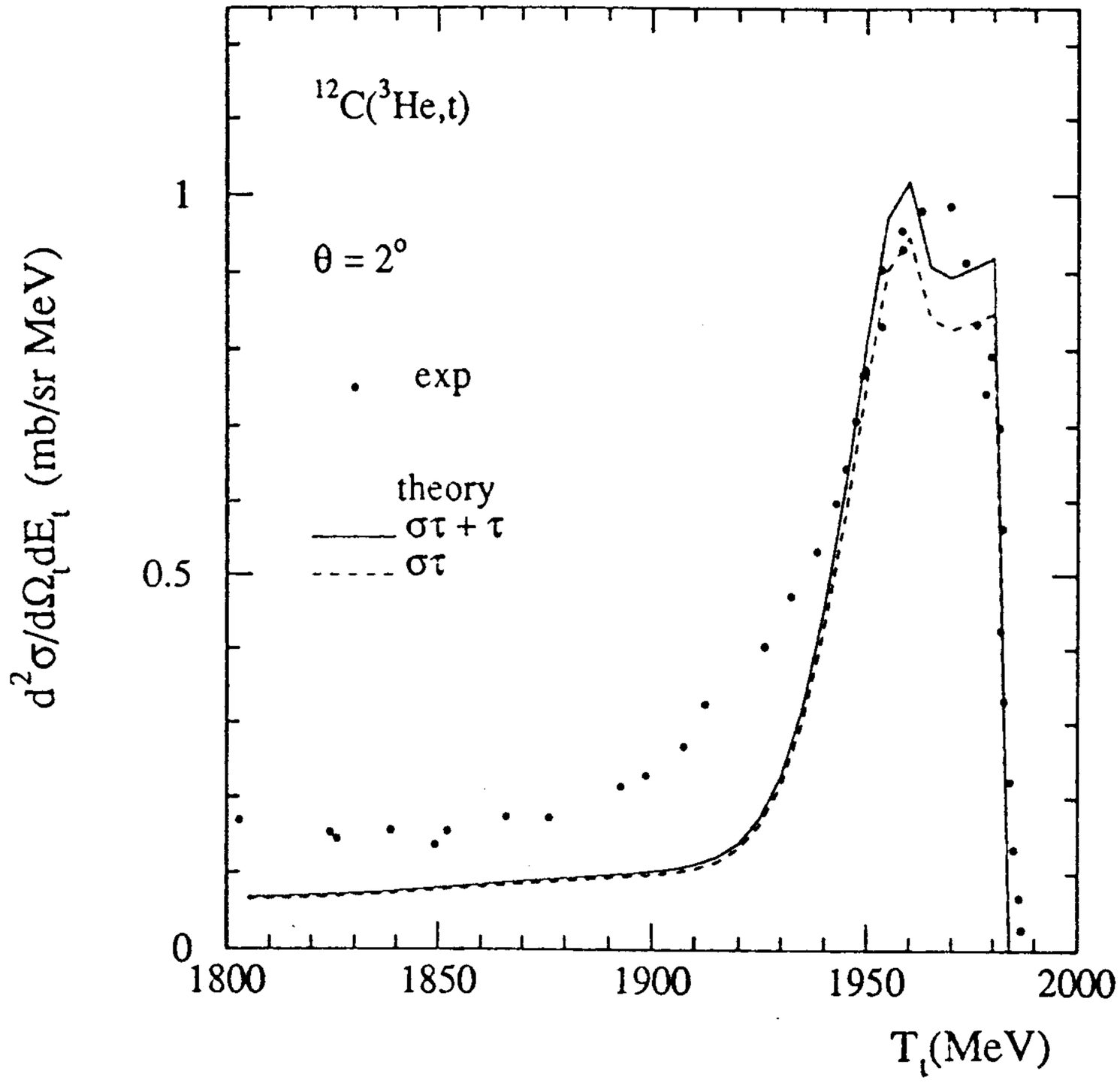

Fig. 9

Comparison of the contribution from the spin-isospin-flip channel (solid curve) and non-spin-flip channel (dashed curve) to the triton energy spectrum at 2° for the $^{12}C(^3He,t)$ reaction at 2 GeV. Dots represent the experimental data (ref.[3]).

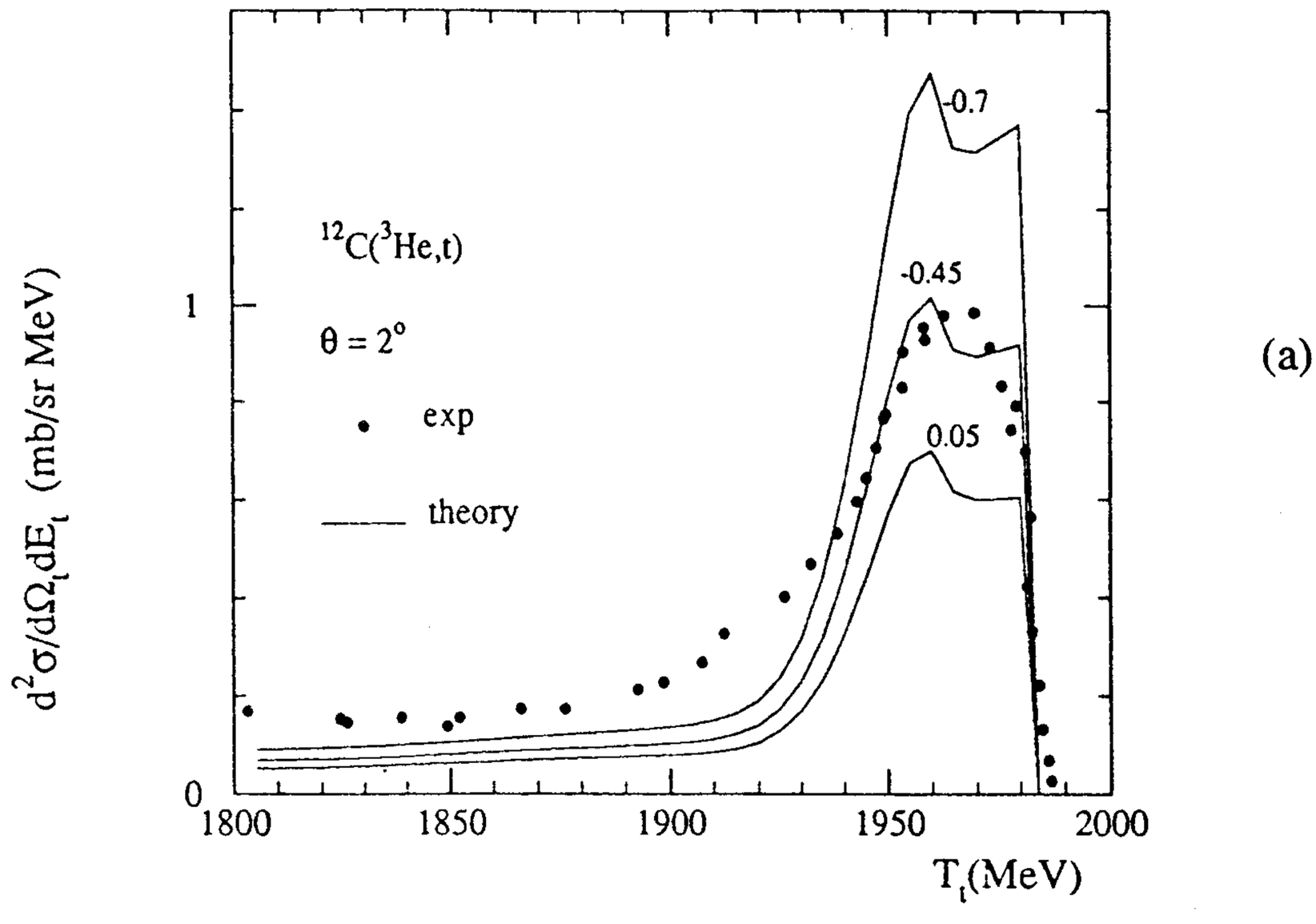

(a)

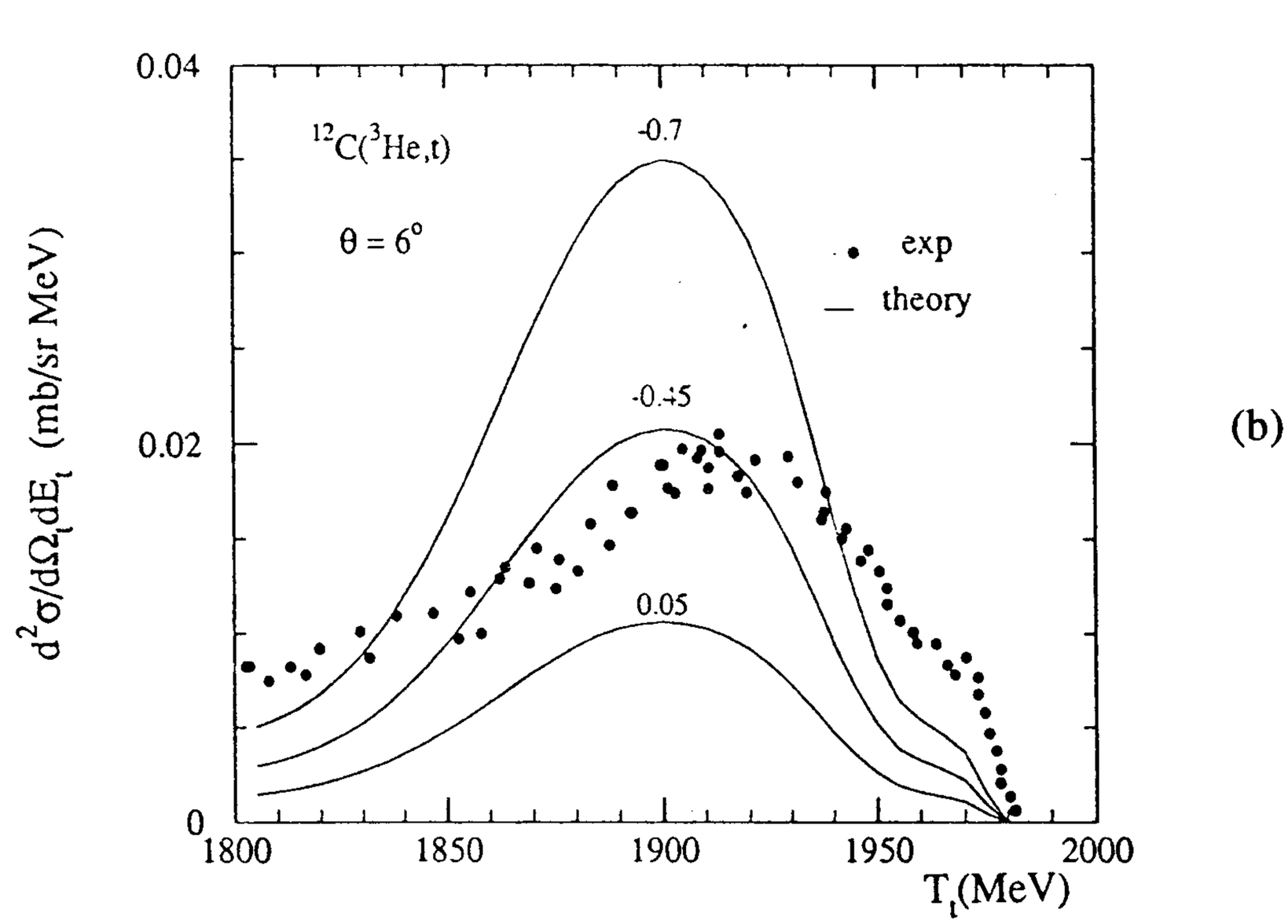

(b)

Fig. 10

Triton energy spectra in the quasielastic peak region at triton angles of 2° and 6° for ^{12}C(^{3}He,t) at 2 GeV beam energy for different values of β. The curves are the cross-sections with the t-matrix consisting of the $\pi + \rho$ exchange transition potential. The numbers on the curves indicate the corresponding values of β.

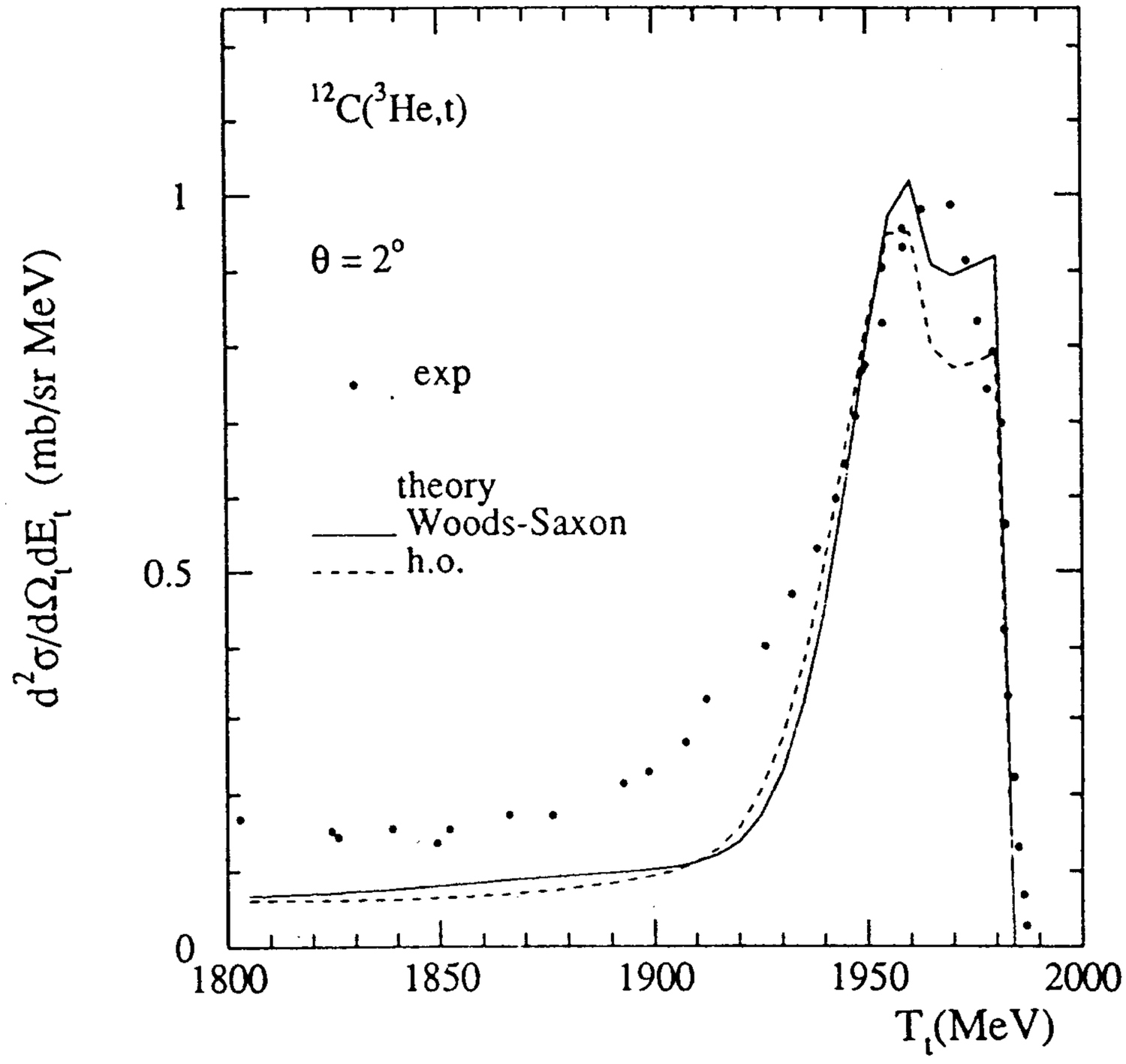

Fig. 11

Triton energy spectrum at triton angle of 2° and 2 GeV beam energy with different forms of the radial wave function ϕ_{nl} of the neutron in the target nucleus.